

Coordinated Fermi/Optical Monitoring of Blazars and the Great 2009 September Gamma-ray Flare of 3C 454.3

P. S. Smith, E. Montiel, S. Rightley, J. Turner, G. D. Schmidt
 Steward Observatory, University of Arizona, Tucson, AZ 85721, USA
 B. T. Jannuzi
 NOAO, Kitt Peak National Observatory, Tucson, AZ 85726, USA

We describe the optical spectropolarimetric monitoring program at Steward Observatory centered around gamma-ray-bright blazars and the LAT Monitored Source List planned for Fermi Cycles 2–4. The large number of measurements made during Cycle 1 of the Fermi mission are available to the research community and the data products are summarized (see <http://james.as.arizona.edu/~psmith/Fermi>). The optical data include spectropolarimetry at a resolution of ~ 20 Å, broad-band polarization and flux measurements, and flux-calibrated spectra spanning 4000–7600 Å. These data provide a comprehensive view of the optical variability of an important sample of objects during the Fermi Era. In addition to broad-band flux and linear polarization monitoring, the spectra allow for the tracking of changes to the spectral index of the synchrotron continuum, importance of non-synchrotron emission features, and how and when the polarization varies with wavelength, an important clue as to the structure of the emission region or the identification of multiple nonthermal components. As an illustration, we present observations of 3C 454.3 obtained in 2009 September during an exceptionally bright gamma-ray flare. The blazar was optically bright during the flare, but except for a few short periods, it showed surprisingly low polarization ($P < 5\%$). Opportunities exist within the Fermi research community to coordinate with our long-term optical monitoring program toward the goal of maximum scientific value to both the Fermi and associated radio VLBI monitoring of blazars.

1. INTRODUCTION

The high apparent luminosity and rapid variability of γ -ray emission observed in blazars [1], lead to straightforward physical arguments implying that, regardless of the mechanism producing the $> \text{MeV}$ photons, the gamma radiation is relativistically beamed as is the bulk of the lower-energy emission [2]. This realization presents the important opportunity during the era of the Fermi Gamma-ray Space Telescope (*Fermi*) to examine for the first time if a direct physical connection can be made between the sites of γ -ray production and those generating the beamed, polarized optical synchrotron continuum in these active galactic nuclei (AGNs). The program at Steward Observatory (SO), described here, is designed to test for this physical connection by providing a unique set of optical linear polarization and flux spectra of blazars.

A fundamental connection between the source(s) of γ -rays and polarization in AGNs is already inferred given that all blazars detected at high energy also show large and similarly variable optical continuum polarization. In addition, polarization measurements provide the only direct means of gaining information on the magnetic field within the synchrotron emission region. The level of linear polarization of a blazar gives a measure of the degree of ordering of the magnetic field within the emission region, and this can be very high (fractional polarization $P \gtrsim 40\%$). The polarization position angle yields the orientation of the field responsible for the polarized flux projected on the sky.

Despite the evidence amassed suggesting that the bulk of the observed emission comes from a single

source - the relativistic jet - it has been generally difficult to find systematic correlations between the variations seen in flux and polarization of different spectral regions (or even within a single spectral region), making it hard to use variability for constraining models of the continuum emission regions. However, optical polarimetry combined with VLBI observations have provided insights about the physical structure and processes involved in generating the powerful and rapidly variable emission in blazars [3], [4], [5].

In the past, it has been nearly impossible to study possible relationships between γ -ray and lower-energy emission in AGNs because of the difficulty in obtaining systematic, high signal-to-noise ratio (S/N) monitoring of sources at high energies. The first year of the *Fermi* mission has changed this situation with the Large Area Telescope (LAT) demonstrating the capability to monitor the 0.1–300 GeV emission for a large sample of AGNs on time scales as short as a day [6], [7].

2. THE OBSERVATIONAL PROGRAM

2.1. Scope of the Monitoring Campaigns

The optical program is designed to nightly monitor γ -ray-bright blazars, both in linear polarization and flux, for about one week every month and to release the data obtained to the research community as quickly as possible. This density of observation provides a good match to the γ -ray variability data that *Fermi* can provide for the brightest blazars in the sky, allowing for the often rapid γ -ray variations to be

directly compared to both the polarization and flux behavior observed for the optical synchrotron continuum. Ideally, optical polarization and flux monitoring should be as continuous as possible, but the number of nights per year devoted to this intensive monitoring at Steward Observatory is constrained by lunar phase, competition from other programs for telescope time, and the increases in manpower that would be required to significantly expand the duration and/or frequency of the observing campaigns. An additional consideration is the substantial effort needed to fully process the polarization, flux, and spectral data described in §3 so that the results publicly presented are definitive. Indeed, an observing campaign uninterrupted by bad weather presents a formidable challenge to fully reduce before the start of the next campaign. The optical program started in 2008 October and is planned to continue until at least the end of Cycle 4 of the *Fermi* mission (2012 August).

During a typical night ~ 20 objects can be observed spectropolarimetrically with the 2.3–1.5 m telescopes available for use. The core of the object sample is the LAT-monitored list of blazars chosen for Cycle 1 of the *Fermi* mission (http://fermi.gsfc.nasa.gov/ssc/data/policy/LAT-Monitored_Sources.html). This sample has been augmented by blazars that have flared in γ -rays during the first year and a half of the mission and announced in Astronomer’s Telegrams (ATELs; http://www-glast.stanford.edu/cgi-bin/pub_rapid) as interesting targets of opportunity. Table 1 listed the blazars that have been observed during the first 11 observing campaigns of the SO program.

2.2. Facilities and Instrumentation

The SO optical program utilizes either the 2.3 m Bok Telescope on Kitt Peak, AZ (<http://james.as.arizona.edu/~psmith/90inch.html>), or the 1.54 m Kuiper Telescope on Mt. Bigelow, AZ (<http://james.as.arizona.edu/~psmith/61inch>). Given that the Kuiper Telescope was designed foremost for planetary and lunar observations, its mount does not allow the telescope to be operated at Declinations north of $\sim +61^\circ$, whereas there is no such restriction with the Bok Telescope.

All observations are obtained using the SPOL spectropolarimeter [8]. SPOL is a versatile, high-throughput ($\sim 30\%$ instrument+telescope), moderate resolution ($R \sim 300\text{--}1000$), dual-beam spectropolarimeter that employs a waveplate and Wollaston prism to modulate and analyze polarized light. A $\lambda/4$ waveplate is inserted into the telescope beam just after the slit to detect circular polarization, a $\lambda/2$ waveplate is used to measurement linear polarization. The instrument is also able to provide imaging polarimetry over a narrow field of view ($\sim 50 \times 50$ arcsec² at

Table I Blazars Observed during the First 11 Observing Campaigns

Object	# Obs.	ΔP (%)	ΔV
3C 66A	21	7.5–19.7	14.05–14.60
AO 0235+164	75	0.6–23.5	15.67–18.79
PKS 0420–014	12	5.8–11.9	16.58–17.21
PKS 0454–123	17	0.2–7.3	...
PKS 0528+134	16	0.8–12.9	19.60–20.87
S5 0716+714	36	2.4–15.5	13.13–14.00
4C 14.23	10	4.4–20.3	...
PKS 0735+178	10	1.6–6.4	16.21–16.45
OJ 248	56	0.1–1.6	17.31–17.54
OJ 287	82	11.6–35.5	14.01–15.63
Mrk 421	72	0.6–6.1	13.05–13.62
PKS 1118–056	15	1.1–22.5	...
H 1219+305	31	1.8–7.5	16.31–16.60
W Com	63	3.3–17.4	14.28–15.31
PKS 1222+216	8	0.8–4.4	15.60–15.90
3C 273	43	0.1–1.5	12.66–12.84
PKS 1244–255	19	0.6–6.9	...
3C 279	49	1.7–34.5	15.31–16.97
PKS 1406–076	6	8.0–17.4	...
H 1426+428	31	0.2–1.8	16.50–16.82
PKS 1502+106	29	5.2–45.2	...
PKS 1510–08	42	1.4–22.6	15.13–17.04
B2 1633+382	45	0.6–7.8	...
3C 345	26	0.8–9.5	16.23–17.39
Mrk 501	67	0.1–5.6	13.84–14.03
GB6 B1700+6834	9	1.9–11.2	...
NRAO 530	6	2.8–6.3	...
1ES 1959+650	40	3.2–8.5	14.61–15.02
PKS 2155–304	45	0.9–10.1	12.87–13.91
BL Lac	86	4.2–25.6	14.67–15.39
CTA 102	11	0.3–1.7	17.08–17.21
3C 454.3	140	0.2–13.8	14.54–16.52
1ES 2344+514	59	0.5–3.4	...

both 2.3 m and 1.5 m telescopes) with the substitution of a diffraction grating by a plane mirror in the light path. The detector is a 1200×800 pixel², thinned, antireflection-coated SITE CCD having $\lesssim 2.5$ e[−] read noise.

The intent of the monitoring program is to provide a comprehensive view (both the flux and polarization *spectra*) of the optical emission from γ -ray-bright blazars for comparison with their high-energy emission as well as with VLBI monitoring at radio wavelengths. Therefore, the default configuration of SPOL employs a 600 l mm^{-1} grating, providing spectral coverage of $4000\text{--}7550 \text{ \AA}$ in first order, with a resolution

of 15–25 Å, depending on the slit width chosen for the observation. Seven slits, each with a length of $\sim 50''$, provide a range of widths from $1''$ – $13''$. Typically, slit widths of $2''$ – $3''$ are used for spectropolarimetry depending on the seeing and the brightness of the target, while the widest slits are utilized for the differential spectrophotometry described in §3.2.

Occasionally, SPOL is configured for imaging polarimetry during an observing campaign. This is usually done on marginal nights when observations need to be completed more quickly during short breaks in the cloud cover. In these cases, the spectral coverage of the measurements are defined by a standard Johnson *V* filter bandpass.

2.3. Calibration

Polarization measured by SPOL is rotated to the conventional astronomical reference frame by observing known interstellar polarization standard stars [9]. At least two standards are observed per campaign as a consistency check. The uncertainty in the absolute calibration of the polarization position angle (θ) from the grid of standards used is not folded into the estimated uncertainty of a measurement. The uncertainties reported for θ are statistical as systematic errors in the absolute calibration would apply equally to all measurements within an observing campaign.

The efficiency of the $\lambda/2$ -waveplate is checked every campaign by inserting a full-polarizing Nicol prism into the beam and measuring the result. The efficiency of the semi-achromatic $\lambda/2$ -waveplate used in SPOL varies between 0.97 at ~ 4500 Å to nearly 1.0 at ~ 6500 Å, before falling back off to 0.97 by ~ 8000 Å. This calibration is applied to all polarization results.

As a check for instrumental polarization, at least one unpolarized standard star [9] is observed per campaign. No correction for instrumental polarization is made to the data as SPOL consistently shows that the polarization imparted by the telescope and instrument is $\lesssim 0.1\%$.

All calibration of the optical flux measurements is from differential flux measurements made using stars in the fields of the targeted blazars. The majority of targets observed since Fermi launch have calibrated field stars (see e.g., [10], [11], [12]), though 10 do not, and as a result, no range in *V* magnitude is given for these objects in Table I. The difference in magnitude between the blazars and the identified comparison star is given whenever differential spectrophotometry is performed, so in principle the apparent magnitude can be recovered in the future if the comparison stars are calibrated.

Optical spectra, usually from the spectropolarimetric measurements, are flux calibrated by observing several spectrophotometric standard stars throughout an observing campaign. An average sensitivity

function is derived from these observations to convert the instrumental spectra to F_λ with units of $\text{erg cm}^{-2} \text{s}^{-1} \text{Å}^{-1}$ over the range $\lambda = 4000$ – 7550 Å. Corrections are applied to the flux density spectra for the airmass of the target during the observation and the elevation of observatory using the standard KPNO extinction curve within the IRAF reduction package (see [13]).

3. THE AVAILABLE DATA PRODUCTS

All of the reduced data obtained during this program are publicly available at <http://james.as.arizona.edu/~psmith/Fermi>.

3.1. Polarimetry

As of the end of campaign #11 (2009 November), almost 1300 polarization measurements of 33 blazars have been made (see Table I). The primary data products of the spectropolarimetry are spectra of the normalized linear polarization Stokes parameters q and u spanning 4000–7550 Å. The median q and u for $\lambda = 5000$ – 7000 Å is determined from the spectra and used to calculate P and θ . All four quantities are summarized in tables both sorted by time and by object, with the measurement uncertainties determined from the RMS measured in the Stokes spectra.

The full-resolution Stokes spectra are also made available in addition to the summary tables so that investigators may bin the spectropolarimetry as desired. Providing the q and u spectra is more straightforward than producing equivalent spectra of P and θ because of the normal error distribution of the Stokes parameters. All reported values of P have been corrected for statistical bias inherent in these measurements [14]. The correction used is

$$P = \sqrt{(q^2 + u^2) - \sigma_p^2}. \quad (1)$$

This correction is insignificant given the very high S/N measurements resulting from binning the spectra over 2000 Å (500 pixels), when typically, $\sigma_p < 0.1\%$ based on photon statistics. However, the measurement bias becomes significant if the spectra are much more finely binned, or for objects that are faint and/or nearly unpolarized.

On occasion, *V*-band imaging polarimetry is obtained instead of spectropolarimetry. As there are no Stokes spectra produced from these observations, the polarimetry is only summarized in the data tables.

3.2. Photometry and Flux Spectra

For clear nights (or clear portions of nights), the results from differential spectrophotometry are summarized in nightly photometry tables. Tables that

summarize entire observing campaigns are also available that sort the photometry by object. These measurements are independent of the spectropolarimetry as they utilize the widest slits available in the instrument to avoid variations in seeing and wavelength-dependent slit losses, especially when a target is observed at a low elevation in the sky. These large-aperture observations yield a flux spectrum of the blazar and one or more comparison stars in the field. After convolving the the flux spectra with a synthetic V filter bandpass, the flux is summed and the magnitude differences computed.

For those fields that have calibrated magnitudes for the comparison stars, the apparent V magnitude of the blazar is reported in the photometry summary tables. For all measurements, the differential magnitude and the identification of the comparison star(s) used are reported so that investigators can revise the reported apparent magnitudes if there are future refinements to the calibration of the field stars, or if a currently uncalibrated field is calibrated in the future.

Since the flux spectra span 4000–7550 Å, both the standard V and R photometric bandpasses are encompassed. By default, the results at V are reported, but the data exist to construct blazar light curves at R as well as any other filter bandpass covered by the spectra. Investigators interested in using the differential spectrophotometry to combine with photometry obtained in filters other than Johnson V should contact the authors to have the appropriate data made available for use.

Flux spectra resulting from the spectropolarimetry are of much higher S/N than the spectra from the large-aperture spectrophotometry because they are the co-addition of 16 exposures taken at various waveplate positions. In contrast, the spectrophotometric spectra are from a single exposure with a much higher sky background because of the wider slit employed. The spectra from the spectropolarimetry are calibrated using the averaged sensitivity function for the observing campaign (see §2.3) and made available so that the optical continuum and any spectral features can be followed and compared with the γ -ray flux variations detected by *Fermi*.

Occasionally, spectra suffer from slit-loss problems when objects are observed at airmasses of 2 or greater since the slit is not oriented at the parallactic angle (the slit is left aligned east-west for all observations so as not to disrupt the calibration of θ). This problem is corrected by closely comparing the continuum shape of the blazar from the narrow-slit observation with that from the wide-slit spectrophotometry, which is insensitive to the effects of differential atmospheric refraction. The final, reduced spectrum is corrected to match the lower- S/N , wide-slit observation. In addition, the flux spectrum is scaled to the results of the synthetic V -band photometry for that night, although this is not done on non-photometric nights or

for objects with no calibrated comparison stars.

For each monitored object, the reduced full-resolution total flux and Stokes (q and u) spectra are available for download in a single gzipped tar file. As of 2009 August, the spectra are complete for all of the optical observations obtained during Cycle 1 of the *Fermi* mission.

4. 3C 454.3 IN 2009 SEPTEMBER

An example of the results from the SO optical monitoring program are given by the observations of 3C 454.3 obtained during a very active period of γ -ray emission in 2009 September (optical campaign #9). Figure 1 shows the optical measurements over a two-week period, along with the 0.1–300 GeV flux as measured by *Fermi*. Error bars are plotted for all of the data, but these are generally smaller than the points denoting the optical photometry and polarimetry. The polarization measurements are determined from the $\lambda = 5000$ – 7000 Å median values of q and u .

In the top panel of Figure 1, a strong correlation can be seen between the γ -ray and optical fluxes, with both reaching a sharp peak on 2009 Sep 17 (UT). The correlation with the γ -ray flux is even more pronounced in polarized flux ($P \times F_\nu$). The polarization generally increases steadily until Sep 17, when $P \sim 12\%$, and then drops to $\sim 3\%$ within a day. In contrast, the polarization position angle only shows large differences with its value on Sep 17 ($\theta \sim 150^\circ$) several days prior to and after the peak of the γ -ray flare.

Although the systematic behavior seen in Figure 1 is highly suggestive of the common region producing the optical and γ -ray photons, even this relatively short time series of observations reveals complications. Note that the high level of polarization observed on MJD = 55098 is not accompanied by an increase in γ -ray flux. Also, large rotations in θ are seen during periods of relatively stable optical and γ -ray emission.

Figure 2 shows the full-resolution optical flux and linear polarization spectra from 2009 Sep 17. In the top panel, the total flux spectrum of Sep 17 is compared to the spectrum of 3C 454.3 obtained on 2009 Jan 30, when the blazar was optically two magnitudes fainter ($V \sim 16.5$) and was not detected by *Fermi* on daily time scales. The polarization of the blazar is not compared for these two epochs since it was essentially unpolarized ($P < 1\%$) on Jan 30.

From Figure 2, it can be seen that the spectroscopic data delivered by the SO monitoring program adds several pieces of important information that are not available from the broad-band measurements. First, the slope of the optical continuum can be measured, which is an important diagnostic for the optically thin synchrotron source producing the polarized flux. Indeed, the spectral index of the polarized flux can be

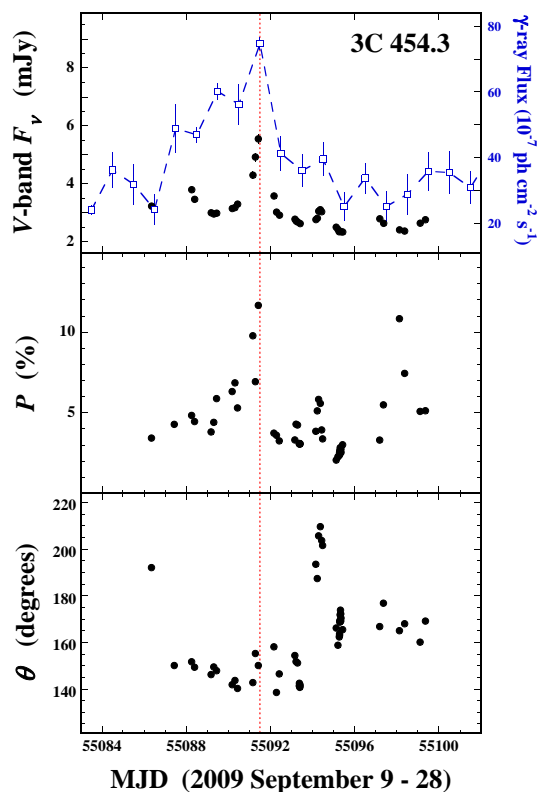


Figure 1: Optical flux and linear polarization measurements of 3C 454.3 obtained during the first major emission peak in the γ -ray light curve at the start of flaring period for the blazar in 2009 September. Gamma-ray fluxes at 0.1–300 GeV are shown in the top panel as open squares connected by *dashed* line segments. The vertical line through all panels denotes the peak γ -ray flux from this period. There is a high degree of correlation between the high-energy flux and both the total and polarized optical fluxes.

determined *independently* of any contribution to the optical spectrum from sources such as the Big Blue Bump (BBB), the host galaxy, and emission lines. Second, the variation with wavelength of the polarization can be measured. Wavelength-dependent P and/or θ is an important diagnostic for the structure of the emission region or for the identification of multiple polarized non-thermal emission regions. Unpolarized flux components, such as starlight from the blazar host galaxy and the BBB, often difficult to detect by analysis of the flux spectrum alone can be uncovered in the spectrum of P [15]. Finally, the strength of emission and absorption features can be monitored over the duration of the SO program in a systematic fashion.

For the case of 3C 454.3 shown in Figure 2, the differences in the flux spectra between bright and faint

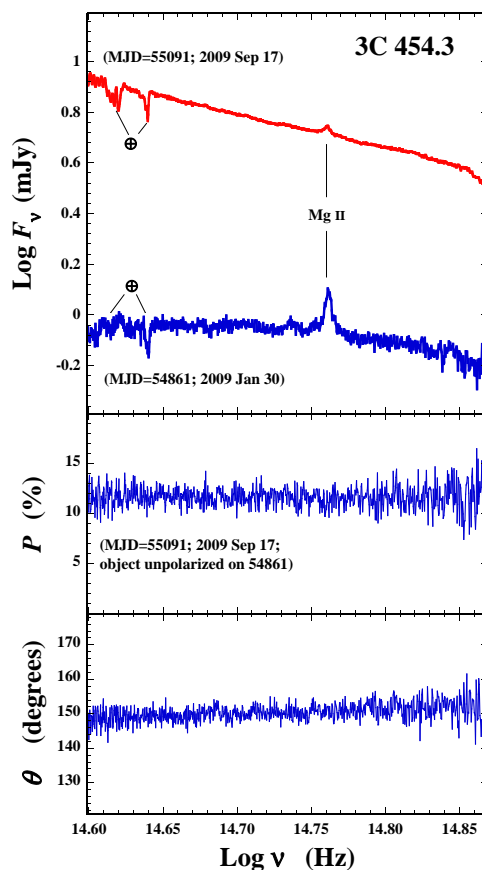


Figure 2: Full-resolution optical flux and linear polarization data obtained on 2009 Sep 17 near the peak of the 0.1–300 GeV flux. In the top panel, the optically bright flux spectrum is compared to that from 2009 Jan 30, when 3C 454.3 was much fainter and essentially unpolarized. (*Fermi* was unable to detect the blazar daily during much of 2009 Jan/Feb.) Also notice that the optical spectrum is much redder when the object is bright, as the steep synchrotron continuum dominates and nearly washes out Mg II. Spectra are shown in the observed frame.

optical and γ -ray periods are readily apparent. The bright optical spectrum is much redder than that of 2009 Jan 30, as the steep power-law synchrotron spectrum dominates the continuum and makes the Mg II emission line much less prominent. The faint optical spectrum is much bluer, presumably because of the dominance of the unpolarized BBB found from observations of the wavelength dependence of P [16]. For this particular example, 3C 454.3 was nearly unpolarized on Jan 30, consistent with the BBB dominating the continuum. The telltale signature for the BBB (P declining in the blue, with θ constant with λ) is, however, seen throughout the SO monitoring program in the polarized spectra of the object during epochs of intermediate brightness.

5. UTILIZING DATA FROM THE SO MONITORING PROGRAM

Researchers are encouraged to contact the Principal Investigator of the SO monitoring program (P. S. Smith; psmith@as.arizona.edu) if they have questions or problems using the data in the public archive for their investigations. Although collaboration is not a condition for use of these data, we request that the source of the observations be cited (and the PI informed by email) in any publication that utilizes results from the Steward Observatory monitoring program. The program is reviewed by the Steward Observatory Telescope Allocation Committee every four months and knowledge of the utility of these observations in the study of blazars helps our ability to garner telescope time for the continuation of the project. Fully collaborative efforts are also encouraged.

Acknowledgments

This work has been made possible by *Fermi* Guest Investigator grant NNX08AV65G. E. Montiel thanks the NASA Space Grant program for an Internship during 2008–09.

References

- [1] Kniffen, D.A., et al. 1993, ApJ, 411, 133
- [2] Urry, C.M., & Padovani, P. 1995, PASP, 107, 803
- [3] Gabuzda, D.C., Rastorgueva, E.A., Smith, P.S., & O’Sullivan, S.P. 2006, MNRAS, 369, 1596
- [4] D’Arcangelo, F.D., et al. 2007, ApJ, 659, L107
- [5] Marscher, A.P., et al. 2008, Nature, 452, 966
- [6] Abdo, A.A., et al. 2009, ApJ, 699, 817
- [7] Abdo, A.A., et al. 2009, ApJS, 183, 46
- [8] Schmidt, G.D., Stockman, H.S., & Smith, P.S. 1992, ApJ, 398, L57
- [9] Schmidt, G.D., Elston, R., & Lupie, O.L. 1992, AJ, 104, 1563
- [10] Raiteri, C.M., Villata, M., Lanteri, L., Cavallone, M., & Sobrito, G. 1998, AApS, 130, 495
- [11] Smith, P.S., & Balonek, T.J. 1998, PASP, 110, 1164
- [12] González-Pérez, J.N, Kidger, M.R., & Martín-Luis, F. 2001, AJ, 122, 2055
- [13] Stone, R.P.S. & Baldwin, J.A. 1983, MNRAS, 204, 347
- [14] Wardle, J.F.C. & Kronberg, P.P. 1974, ApJ, 194, 249
- [15] Smith, P.S., Balonek, T.J., Heckert, P.A., & Elston, R. 1986, ApJ, 305, 484
- [16] Smith, P.S., Elston, R., Berriman, G., Allen, R.G., & Balonek, T.J. 1988, ApJ, 326, L39